

## X-Ray Photoelectron Spectroscopy Study of Silica-Alumina Catalysts Used for a New Pyridine Synthesis<sup>1</sup>

R. BICKER,\* H. DEGER,\* W. HERZOG,\* K. RIESER,† H. PULM,‡ G. HOHLNEICHER,‡  
AND H.-J. FREUND‡<sup>2</sup>

\*Hoechst A.G., 6230 Frankfurt-am-Main 80, Germany; †Grace GmbH, 6520 Worms, West Germany; and  
‡Institut für Organische Chemie, Universität zu Köln, Greinstrasse 4, 5000 Köln 41, West Germany

Received August 2, 1984; revised December 31, 1984

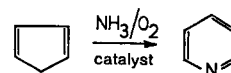
Alumina-doped silica gels used as catalysts for a new pyridine synthesis from cyclopentadiene and ammonia have been investigated using X-ray photoelectron spectroscopy. Two different types of aluminum species are identified. Their chemical nature is assigned to a "normal" Al oxide and a more electron-rich Al species (Brønsted centers). The distribution of the two species within the samples as a function of distance from the surface is not homogeneous and is strongly dependent upon the preparation of the catalyst. The concentration of the Brønsted centers in the proximity of the catalyst surface seems to correlate with the activity of the catalyst in the pyridine synthesis. © 1985 Academic Press, Inc.

### INTRODUCTION

Pyridine, a valuable intermediate in a variety of industrial processes, is manufactured today either by fractional distillation of coal tar or by condensation of acetaldehyde and ammonia (1). These technical routes for the production of pyridine are limited. For example, coal tar contains only little (0.1%) pyridine, and its isolation and purification are difficult and very expensive. In addition coking plants are disappearing more and more since the demand for coke and coking gas is decreasing. In the aldehyde-ammonia process the formation of pyridine is always accompanied by side products (picolines, lutidine, collidine) which limit the economical feasibility of this process.

As an alternative to these processes we have investigated the heterogeneously catalyzed formation of pyridine from cyclopentadiene (2). The latter hydrocarbon is readily

available at low cost from the C<sub>5</sub>-cut of refined oil:



A variety of catalysts have been examined. Alumina-doped silica gels were found to be most active in this process. The catalysts were prepared by incorporating aluminum salts during silica gel formation. Their activity could be varied by adding the salts during different stages of silica gel development. In order to characterize the catalyst and to investigate the chemical state of the aluminum, which is possibly the active metal species, we have applied X-ray photoelectron spectroscopy (XPS). In contrast to other methods often used, (such as IR spectroscopy (3) and titration methods (4)), XPS allows one to specify directly in a surface sensitive manner the "chemical state" of the operative metal species in the vicinity of the catalyst surface. The present paper is intended to give preliminary experimental hints about the chemical nature of the metal species and to trigger further experimental work on these materials.

The paper is organized as follows. We

<sup>1</sup> Dedicated to Prof. Dr. R. Sammet on the occasion of his 65th birthday.

<sup>2</sup> To whom correspondence should be addressed. Permanent address: Institut für Physikalische und Theoretische Chemie der Universität Erlangen-Nürnberg, Egerlandstr. 3, 8520 Erlangen, Germany.

first briefly present the experimental conditions of the study and the applied procedures. In a second part the results are outlined and discussed with respect to an identification of the active species. A final part summarizes the conclusions of our study.

#### EXPERIMENTAL

The pyridine synthesis was carried out in a stainless-steel reactor (16 × 70 mm) filled with the catalyst (pellets, 2-mm diam.). The reactor was heated in a salt bath ( $T = 300^{\circ}\text{C}$ ) and exposed to a gas stream consisting of cyclopentadiene (0.4 g/h)/ $\text{NH}_3$  (5 liters/h)/ $\text{H}_2\text{O}$  (10 g/h)/air (7.5 liters/h). The gas was analyzed by gas chromatography ( $210^{\circ}\text{C}$ , 1.5-m Purpak QS column) before and after the reaction. From the difference the yield of pyridine was determined.

Photoelectron and Auger spectra were recorded using a modified Leybold-Heraeus LHS 10 electron spectrometer in the  $\Delta E/E = \text{constant}$  mode (5). The X-ray tube was equipped with a Si anode (6) (1739.5 eV) to allow ionization of Al 1s electrons. For characterization purposes we compare in Fig. 1 the Si  $K\alpha$ - and Mg  $K\alpha$ -excited spectra of a gold foil in the region of the Au

4f spin-orbit doublet. Although the separation of the two components of Si  $K\alpha$  radiation is larger than for Mg  $K\alpha$  radiation the observed shapes of the Au 4f doublets are identical. Differences appear at lower binding energies due to the different satellite lines associated with Si  $K\alpha$  radiation as compared to Mg  $K\alpha$  radiation.

The spectrometer is interfaced (7) with a PDP 11/10 computer (Digital Equipment). Data were taken every 0.1 eV with a dwell time of 2 s/channel. To keep the signal to a reasonable noise level, spectra were averaged up to 150 scans/spectrum in those cases in which signals of small intensities are of significance. The spectrometer energy scale was calibrated using the known binding energies of Au 4f and Cu 2p (8). Charging was checked upon using previously described methods (9, 10). To analyze our data, however, we use the Auger parameter which is independent of sample charging.

The silica-alumina catalysts were prepared by incorporating aluminum via aluminum salts into the silica gel during different stages of the silica gel development. Some of the dry catalysts prepared in this way were annealed at  $300^{\circ}\text{C}$ . The stage of silica gel development during which aluminum is doped and the amount of incorporated aluminum govern the activity of these silica-alumina catalysts, as seen in Table 1. We refer to the samples by the roman numerals given in Table 1. The relative activities of the samples are

$$\text{II} < \text{IV} < \text{V} < \text{I} < \text{III} < \text{VI}.$$

The activity of VII has not been measured.

Samples V and VII were prepared by annealing samples IV and VI at  $300^{\circ}\text{C}$  for 24 h. This procedure has been applied to study the effect of loss of volatile components of the catalysts on the observed spectra. As reference we used the metal and oxide signals of an oxidized aluminum foil.

The silica-aluminas of types I to V were studied as received. In particular they have not been sputtered before recording the

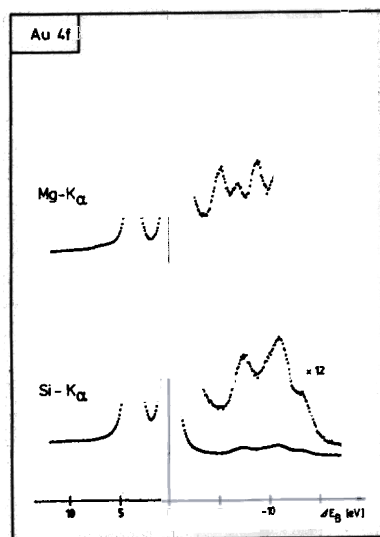


FIG. 1. Mg  $K\alpha$  (1254.6 eV)- and Si  $K\alpha$  (1739.5 eV)-induced Au 4f spectra of a polycrystalline gold foil. The Au  $4f_{7/2}$ -line maximum is given as energy zero.

TABLE 1  
Characterization of Catalyst Samples

No. <sup>a</sup>	Amount of Al (Al <sub>2</sub> O <sub>3</sub> ) (%)	Yield of pyridine (%)	Stage of doping the aluminum
I (1)	2.2	36.7	During an intermediate stage before the development of the internal silica gel structure
	6.5	20.7	During an early stage of the silica gel development
III (3)	1.2	45.5	During a late stage after the development of the internal silica gel structure
	3.8	27.2	During an intermediate stage before the development of the internal silica gel structure
V	3.8	36.1	No. IV heated 24 h at 300°C
VI (5)	0.9	49.5	During a late stage after the development of the internal silica gel structure
VII	0.9		No. VI heated 24 h at 300°C

Note. The Al contents in the silica gels are determined as Al<sub>2</sub>O<sub>3</sub>. The last column contains specific remarks on the individual preparation of the sample before spectroscopic study.

<sup>a</sup> Silica-alumina cogels from Grace GmbH, Worms; (1) No. 4, (3) No. 10, (5) No. 8, (2) No. 3, (4) No. 6.

spectra. Figure 2 shows a 200-eV-wide scan of the region of Si 2s, Si 2p, and Al 2p signals to illustrate the relative signal intensities of Si and Al ionizations. The reproduced spectrum reflects the relative amount of Al and Si within the escape depth of sample II, which contained the largest amount of alu-

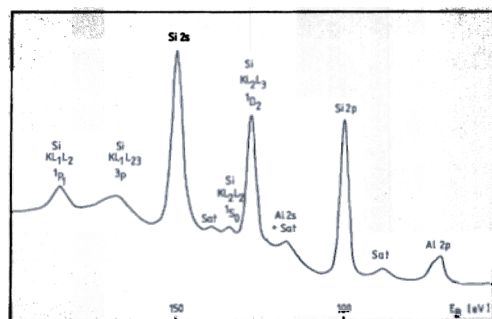


FIG. 2. Wide scan (200 eV) of a representative sample (II) below 50-eV binding energy. The peaks induced by the X-ray satellites of the source are marked by "Sat." The peaks of the Si KLL Auger spectrum are characterized by their term symbols.

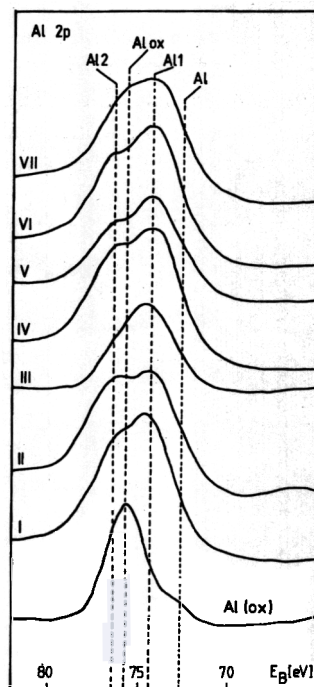


FIG. 3. Al 2p spectra of samples I-VII. The peak areas have not been normalized. For comparison a spectrum of an oxidized Al foil (Al(ox)) is shown at the bottom.

minum. Our discussion in the next section is restricted to the electronic structure of the aluminum sites. Therefore we show in Figs. 3-5 the Al 1s, Al 2p, and the most intense peaks of the Al KLL photoinduced Auger spectrum (14) of samples I to VII. We include for comparison the spectra of an oxidized Al foil. Figure 6 shows the full photoinduced Al KLL spectrum of the oxidized aluminum foil, excluding the 'S' state at lowest energy originating from the 2s<sup>0</sup>2p<sup>6</sup> double-hole-state configuration.

## RESULTS AND DISCUSSION

Figure 3 shows the spectra of the Al 2p signals as determined for samples I to VII together with the signal of the oxidized aluminum foil which is included at the bottom of Fig. 3.

Before discussing the spectra of Fig. 3 we note that ionization of a 2p electron out of a

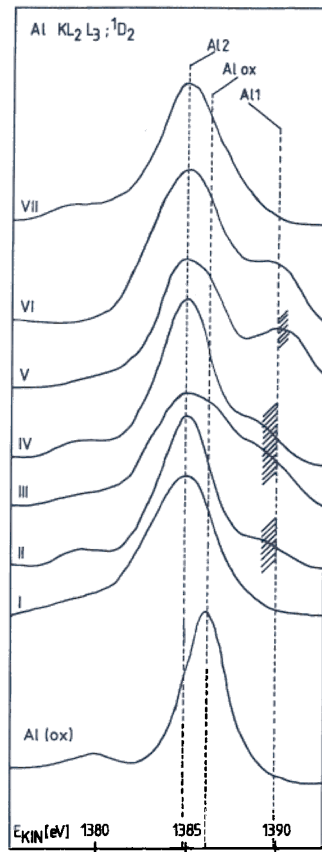


FIG. 4. Al  $KL_2L_3 \ ^1D_2$  Auger spectra of samples I-VII. The peak areas have not been normalized. For comparison a spectrum of an oxidized Al foil (Al(ox)) is shown at the bottom.

filled  $2p$  shell leads to two final states with total spin  $\frac{1}{2}$  and  $\frac{3}{2}$  ( $2p_{1/2}$  and  $2p_{3/2}$ ) and intensity ratio  $2p_{1/2}/2p_{3/2} = \frac{1}{2}$ . The splitting of these two states, however, is  $E_{1/2,3/2} = 0.4$  eV (11) and cannot be resolved with the chosen spectrometer setting, which allows for a resolution of 1.5 eV. Therefore the two lines observed for the oxidized foil are due to two different chemical species, namely ionization of metallic aluminum (Al) at 72.8 eV and aluminum oxide (Al<sub>ox</sub>) at 76-eV binding energies. Satellite structure can be excluded since the relative intensity of the two lines depends on the chemical composition of the sample, which can be varied by sputtering. Upon comparison of the Al  $2p$  spectra of our samples I to

VII with the spectrum of the oxidized Al foil it is obvious that those spectra exhibit linewidths much too large to be due to a single species. Clearly, spectra I, II, IV, V, and VI indicate a doublet structure. The positions of the two most important components are marked Al 1 and Al 2. They do not coincide with metallic aluminum (Al) and aluminum oxide (Al<sub>ox</sub>). Al 1 has a binding energy of 74.4 eV, intermediate between metallic aluminum and aluminum oxide. Al 2 has a binding energy of 76.8 eV, which is greater than that of aluminum oxide. Although the spectra of samples III and VII do not show a pronounced doublet structure the widths of the signals is consistent with the superposition of spectra of two (or more) different chemical species in the energy range between 73- and 77-eV binding energy. Particularly, spectrum II seems to indicate that there is relatively more of Al 2 present in the probed surface

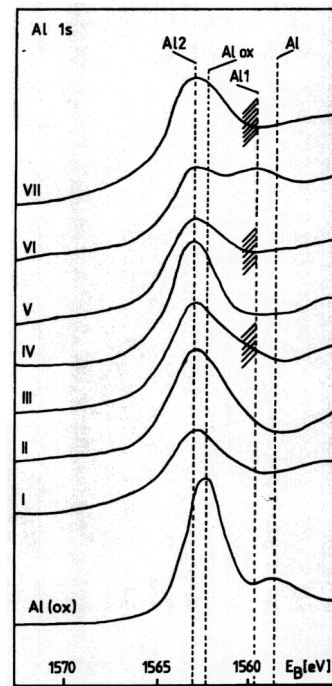


FIG. 5. Al  $1s$  spectra of samples I-VII. The peak areas have not been normalized. For comparison a spectrum of an oxidized Al foil (Al(ox)) is shown at the bottom.

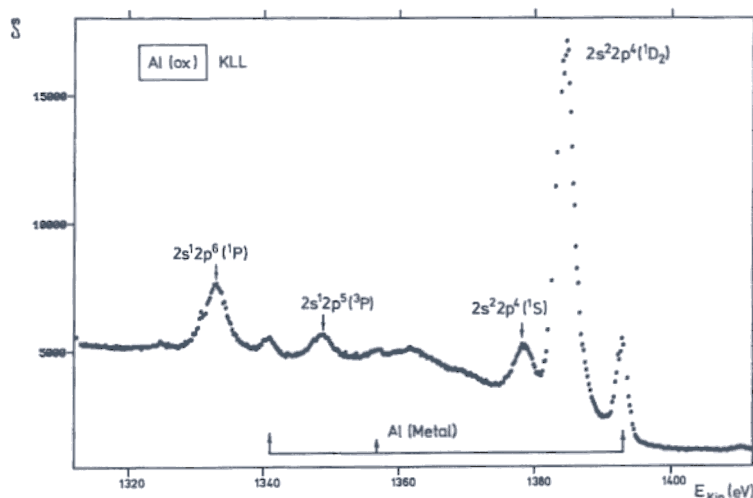


FIG. 6. Al KLL Auger spectrum of a sputtered oxidized Al foil. The peaks are assigned by their term symbols.

region with depth of approximately 20 Å. In addition, if we measure the aluminum content using the  $(\text{Al } 2p)/(\text{Si } 2p)$  intensity ratio (corrected for differences in cross section (15) we find, e.g., for samples I, II, and VI: 0.24, 0.30, and 0.20, respectively. These values deviate considerably from those for the bulk (Table 1). Although one has to use this quantitative information with caution we conclude that within the probed sample volume the concentration of Al is higher than expected from the bulk values.

In order to obtain further evidence about the chemical nature and number of species involved in the spectra, we recorded the Al KLL spectra of all samples. The data are collected in Fig. 4. Again the spectrum of the oxidized aluminum foil is shown at the bottom of the figure. Note that the energy scale now refers to the kinetic energy of the Auger electrons (14). To point out clearly the part of the Al KLL spectrum to which we refer, Fig. 6 shows a more complete spectrum of an oxidized aluminum foil which has been sputtered slightly longer than the one which leads to the spectrum in Fig. 4. Due to the reduced escape depth of electrons with approximately 1400-eV kinetic energy ( $\sim 15$  Å), a more extended

cleaning process was necessary to produce an Auger spectrum which shows the peaks of both aluminum metal and oxide.

The assignment given in Fig. 6 is straightforward on the basis of literature data (12, 14) and it is not appropriate to discuss it in this context. We shall only compare in the following the most intense multiplet component, marked as  $^1D_2$ , originating from the configuration  $\text{Al } 2s^2 2p^4$  (14). The important point is that the chemical shift between the metal  $^1D_2$  state and the corresponding peak of the oxide is 7.2 eV, in agreement with data from the literature (12). This is larger by a factor of 2 than the chemical shift observed for Al 2p hole states. Briefly, this enhanced shift is a consequence of increased screening in the final double-hole state of the system (16).

If we return to Fig. 4 we find that the Auger spectra ( $^1D_2$  band) of the samples exhibit two bands (with the exception of I and VII with only one band) which do not coincide with  $\text{Al}_{\text{ox}}$  and Al (which is not even on the energy scale of the section shown). According to their energy positions the lines have to be assigned to Al 2, which is the most intense one at low kinetic energies, and to Al 1 which is situated at higher ki-

netic energies. The chemical shift between the two species is now approximately 5 eV, which is about 2 eV more than observed for the Al 2*p* hole states. The intensities of the two component bands vary rather strongly with sample preparation. As stated before, Al 1 is not observable for VII and I while it seems to be most intense for III. The shaded areas in Fig. 4 attached to the dashed Al 1 line are included to indicate that the energy position of the Al 2 band is not as uniform as was suggested from the analysis of Fig. 3. With the higher sensitivity of the Auger final state to chemical shifts this can be resolved. For II, III, and IV the shift is slightly smaller, and for V it is slightly larger, than is indicated by the dashed line. Spectrum III seems to indicate that there is possibly some Al<sub>ox</sub> present in the probed region of the sample volume. The relative intensities of Al 1 and Al 2 as observed in Auger electron spectroscopy (AES) are different from the relative intensities in XPS. There are several reasons for this behavior which are hard to separate. Thus, the sample is inhomogeneous and even a small reduction in escape depth for Al KLL in comparison to Al 2*p* may contribute to the observed changes. In addition, it is known (15) that lineshape changes observed for Auger signals of a specific element can influence relative intensities. We note, however, that samples with high Al 1 intensities in Fig. 3 also exhibit the largest Al 1 signal in the Auger spectra. In this study the Auger signal intensities are not of primary interest. The important information is the relative chemical shift of the Auger signal in comparison with Al 2*p* chemical shifts as observed by XPS to determine the chemical nature of the species giving rise to Al 1 and Al 2 signals.

To obtain information on the distribution of Al 1 and Al 2 we use the Al 1*s* spectra shown in Fig. 5 in comparison with the Al 2*p* spectra in Fig. 3. For reference purposes the spectrum of a sputtered, oxidized Al foil is shown at the bottom of Fig. 5. The binding energies are in the range 1550 to

1570 eV. The kinetic energy of the photoelectrons is therefore between 150 and 200 eV. With respect to the Al 2*p* spectra this means a considerable reduction in escape depth (to a value below 10 Å). It is clear that the predominant species is Al 2. In fact, a significant amount of Al 1 is only present in sample VI, and some is indicated in sample III. Obviously the topmost surface region is free of Al 1 in most cases.

Before we discuss the results of our measurements in connection with the catalytic activity of the samples, let us try to identify the chemical nature of the two species, so far only characterized as Al 1 and Al 2. This can be done by comparison with spectra of a variety of other aluminum-containing materials using the two-dimensional plot in Fig. 7. This method has been put forward by Wagner (17, 18). The binding energies of the Al 2*p* bands are plotted versus the measured kinetic energies of the Al KLL <sup>1</sup>D<sub>2</sub> Auger band. The diagonal lines refer to the right-hand ordinate where the modified Auger parameter  $\alpha$ , as defined by Wagner (17,

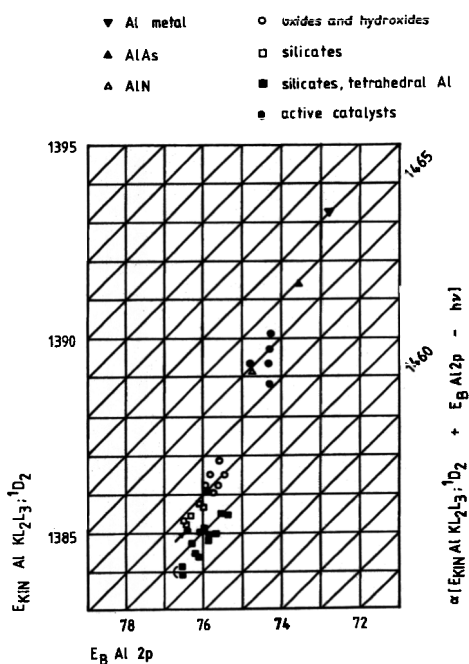


FIG. 7. Chemical state plot of aluminum-containing materials as taken from Ref. (19) with the differences discussed in the text.

18), is plotted.  $\alpha$  is defined as the difference between the Auger kinetic energy and the photoelectron kinetic energy. In order to avoid sign changes in this parameter, depending on whether the kinetic energy of the Auger electron or the kinetic energy of the photoelectron is the larger absolute number, the difference is always added to the photon energy  $h\nu$ .  $\alpha$  is constant along the diagonal lines and has the advantage of being free from charging effects, since both photoelectron kinetic energy and Auger electron energy are influenced by the same surface potential if taken on the same sample. In other words, in the presence of charging the data points move along the diagonal. Most of the entries [36] shown in Fig. 7 have been taken from Wagner *et al.* (19). The values taken from the present work are also indicated as filled circles. Disregarding our own values, Fig. 7 is a reproduction of Fig. 1 and 4 in Ref. (19) with one difference. We have shifted all entries except the ones for AlN and AlAs with respect to abscissa and ordinate along the diagonal in such a way that the binding energy separation between oxidized and metallic aluminum agrees with our results (3.2 eV) of Fig. 3. The binding energy separation between Al and  $\text{Al}_{\text{ox}}$  shown in our spectrum is in agreement with literature data (12, 20). This inconsistency in Fig. 1 of Ref. (19) has also been recognized by Wagner (21). This point is not important for the future analysis but is mentioned here for completeness.

Let us now turn to the details of Fig. 7. The entries fall into three groups, namely around 76-eV binding energy, between 73- and 75-eV binding energy, and metallic aluminum below 73-eV binding energy. The group around 76-eV binding energy falls into two subgroups, the tetrahedrally coordinated aluminum centers in aluminum silicates (■), namely zeolites, with an Auger parameter between 1460 and 1461 eV and octahedrally coordinated aluminum centers in oxides, hydroxides (○), and silicates (□) with an Auger parameter around 1462 eV

(19). The binding energy derived from aluminum oxide layers on top of metallic aluminum is shown as a filled circle (●) within the region of aluminum oxides, i.e., octahedrally coordinated aluminum. The Al 2 species with an Auger parameter of 1461.5 eV (filled circle with arrow) is found in the region of octahedrally coordinated aluminum in silicates as expected. Since the values for Al 2 are almost independent of sample preparation the single entry represents the values for all samples. The values for Al 1 lie within the second group of values above 74-eV binding energy and vary with respect to the Auger parameter within a range of slightly more than 1 eV. Five entries are presented because for the other two samples an Auger peak could not be observed, as pointed out in connection with Fig. 5. The variation of the Auger parameter clearly shows that Al 1 does not represent a single unique chemical species, while Al 2 could be suspected to be unique. Note that Al 1 and Al 2 originate from one sample, which means that there are definitely two different chemical species present, while for the other aluminum-containing materials only one line has been observed, except with H-Zeolon (marked with a curved bracket). In the latter case the line was broader, so that two species might have been present (19, 21).

Having thus established the different nature of Al 1 and Al 2 we can use Fig. 7 to draw conclusions about the electronic charge on the aluminum centers Al 1 and Al 2. This cannot be done by just using the difference in binding energy of the Al 2p lines, because the observed shift in the spectrum is a superposition of initial-state (electronic charge) and final-state effects, as discussed by various authors (22). The Auger parameter, however, which is independent of sample charging, can be used to determine in an approximate manner the contribution of the final state. This has been shown by Wagner *et al.* (17, 18), Wertheim *et al.* (23), and recently by Pulm *et al.* (6, 24). The difference between the observed

Auger parameter and a reference value, for which we use the Auger parameter of metallic aluminum, is approximately equal to twice the relaxation contribution to the shift. Since relaxation always stabilizes the final state, the observed shift has to be reduced by the relaxation contribution. Applying this procedure to our data we end up with binding energy differences due to initial-state effects as shown in Table 2.

On the basis of Table 2 Al 1 obviously carries a higher electron density than Al 2. Since our samples only contain silicon, aluminum, oxygen, and hydrogen we conclude from Fig. 7 that Al 2 is due to photoemission from oxygen-coordinated aluminum centers. It is not clear whether the aluminum centers are octahedrally or tetrahedrally coordinated although the observed Auger parameter is closer to the one found for octahedrally coordinated aluminum centers in silicates. For the species that gives rise to the Al 1 emission we propose aluminum centers of Brønsted type. Clearly, this assignment can only be tentatively based solely on our XPS results. The application of other experimental techniques is highly desirable to provide further conclusive evidence. However, the assignment of Al 2 to a species whose chemical nature is different from an oxide center (Al 2) is reasonable considering the difference in the observed Auger parameter. The Brønsted centers are formed from

the reaction of aluminum centers in three-fold oxygen coordination with hydroxyl ions from water (25). If the OH bond dissociates, the remaining oxygen ion is only coordinated to one aluminum atom and can donate more electron density toward the aluminum atom. This in turn leads to the smaller chemical shift with respect to metallic aluminum.

Summarizing the spectroscopic analysis so far, we find evidence for the presence of two different aluminum species, which can be identified as the "normal" octahedrally coordinated aluminum oxide species usually found in silicates, and an electron-rich species, tentatively assigned to Brønsted centers. The distribution of the two observed aluminum species as a function of distance from the surface is not homogeneous. The presence of the Brønsted centers in the proximity of the sample surface strongly depends on the preparation procedure of the catalyst material. The amount of Brønsted centers close to the surface does not scale with the amount of aluminum in the sample. In fact, almost the inverse is true. Sample VI which was impregnated with the smallest amount of aluminum shows the largest Brønsted aluminum signal in the Al 1s spectrum, indicating a high concentration close to the sample surface. This same sample leads to the highest pyridine yield in the catalyzed reaction as shown in Table 1. Sample III with second lowest aluminum load shows the most asymmetric peak in Fig. 5 and we suspect a rather high Brønsted center concentration in surface proximity. Again, this sample leads to a rather high pyridine yield.

We therefore deduce from our study, qualitatively that there is a correlation between catalyst activity and Al 1 concentration in the surface region. Figure 5 allows us to draw this conclusion since in this case only a small region below the sample surface is probed while for the spectra shown in Fig. 3 the escape depth of the measured electrons is too large to give us the relevant information directly. Figure 3 leads via Fig.

TABLE 2

Contribution of the Electron Density Difference in the Neutral Ground States to the Shift in Binding Energy Observed in the XPS Experiment

Species	Shift (eV)
Al <sub>met</sub>	0.0
Al 2	2.6
Al 1a	1.02
Al 1b	0.98
Al 1c	1.35
Al 1d	0.97
Al 1e	0.98

7 to an identification of the chemical nature of the involved species. To what extent the presence of the second observed chemical aluminum species besides the Brønsted centers are relevant to the catalytic process cannot be deduced from this study. Usually it is assumed, however, that a single type of catalytic center is active in processes on aluminosilicate surfaces (25).

The mechanism of the catalytic process, and in particular the question about the species that is produced by interaction of ammonia and/or cyclopentadiene with the aluminosilicate surface, cannot be answered from the study presented here. It is suspected, however, from infrared studies that, by interaction of NH<sub>3</sub> with Brønsted centers on aluminosilicates, ammonium ions are formed (25, 26). These ions may attack the  $\pi$ -system of the carbon-ring system so that the pyridine heterocycle can be formed.

#### CONCLUSIONS

We have presented results of an X-ray photoelectron spectroscopic study of silica-alumina catalysts used for a new pyridine synthesis. The results indicate the presence of two different types of aluminum species which are distributed with different depth profiles within the catalysts. The chemical nature of the two species is identified as "normal" aluminum oxide centers and species with higher electron density on the metal center. We tentatively assign the latter species to Brønsted centers. The concentration of the Brønsted centers in the proximity of the catalyst surface seems to correlate with the activity of the catalysts in the pyridine synthesis.

The results of our study explain why a low loading of aluminum is sufficient to yield high pyridine yields when we choose the silica gel phase after development of its internal structure for doping the aluminum.

A higher aluminum loading at an earlier development stage of the silica gel obviously influences the incorporation of the aluminum into the gel in a way that is unfavor-

able to yield high Brønsted center concentration close to the catalyst surface.

#### ACKNOWLEDGMENT

The Hoechst group kindly thanks Professor H. Jensen for continuous support of this work. H.J.F. thanks the "Fonds der Chemischen Industrie" for financial support.

#### REFERENCES

1. Budzinski, H., *Chem. Ind. (London)* **33**, 529 (1981); Beschke, H., *Aldrichimica Acta* **14**, 13 (1981); Beschke, H., and Friederich, H., *Chem.-Ztg.* **101**, 377 (1977); Beschke, H., and Kleemann, A., "Ullmanns Encyclopädie der Technischen Chemie," Vol. 19, p. 591. Verlag Chemie, Weinheim, 1981.
2. EP 46897 (Hoechst AG); DOS 32 44 032 (Hoechst AG).
3. Umehara, M., Oda, T., Ikebe, Y., and Hishida, S., *Bull. Chem. Soc. Jpn.* **49**, 1078 (1976).
4. Buchholz, H., Luttmann, R., Zakrzewski, W., and Schügerl, K., *J. Chem. Technol. Biotechnol.* **31**, 435 (1981).
5. Pollaschegg, H. D., *Appl. Phosp.* **4**, 63 (1974).
6. Pulm, H., thesis. Köln, 1984.
7. Gonska, H., and Baum, H. G., unpublished.
8. Johannson, G., Hedman, J., Berndsson, A., Klasson, M., and Nilsson, R., *J. Electron Spectrosc. Relat. Phenom.* **2**, 295 (1973).
9. Freund, H.-J., Gonska, H., Lohneis, H., and Hohlneicher, G., *J. Electron Spectrosc. Relat. Phenom.* **12**, 425 (1977).
10. Gonska, H., Freund, H.-J., and Hohlneicher, G., *J. Electron Spectrosc. Relat. Phenom.* **12**, 435 (1977).
11. Eberhardt, W., Kaloffen, G., and Kunz, C., *Solid State Commun.* **32**, 901 (1979).
12. Castle, J. E., and Wert, R.H., *J. Electron Spectrosc. Relat. Phenom.* **18**, 355 (1980).
13. Ertl, G., and Küppers, J., "Low Energy Electrons and Surface Chemistry" (H. F. Ebel, Ed.), Monographs in Modern Chemistry. Verlag Chemie, Weinheim, 1974.
14. Sevier, K. D., "Low Energy Electron Spectroscopy." Wiley, New York, 1972.
15. Briggs, D., and Reviere, J. C., in "Practical Surface Analysis by Auger and XPS" (D. Briggs and M. P. Seah, Eds.). Wiley, New York, 1983.
16. Aksela, S., *J. Electron Spectrosc. Relat. Phenom.* **24**, 91 (1981).
17. Wagner, C. D., *Faraday Discuss. Chem. Soc.* **60**, 291 (1975).
18. Wagner, C. D., *J. Electron Spectrosc. Relat. Phenom.* **10**, 305 (1977).
19. Wagner, C. D., Passoja, D. E., Hillery, H. F., Kinisky, T. G., Six, H. A., Jansen, W. T., and Taylor, J. A., *J. Vac. Sci. Technol.* **21**, 933 (1982).

20. Taylor, J. A., *J. Vac. Sci. Technol.* **20**, 751 (1982).
21. Wagner, C. D., private communication.
22. Freund, H.-J., *Habilitationschrift*, Köln, 1983; and references therein.
23. Wertheim, G. K., Cohen, R. C., Crecelins, G., Wert, K. W., and Werwick, J. H., *Phys. Rev.* **320**, 860 (1979).
24. Pulm, H., Hohlneicher, G., Freund, H.-J., Schuster, H. U., Drews, J., and Eberz, U., *Less Common Metals*, in press; G. Hohlneicher, H. Pulm, H.-J. Freund, to be published.
25. Schlosser, E. G., "Heterogene Katalyse," "Chemische Taschenbücher," Vol. 18. Verlag Chemie, Weinheim, 1972.
26. Boehm, H. P., "Advances in Catalysis," Vol. 16, p. 179. Academic Press, New York, 1966.